JOURNAL OF APPLIED ELECTROCHEMISTRY **26** (1996) 865–872

Modelling electrode transients: the strongly implicit procedure

J. A. ALDEN, R. G. COMPTON*, R. A. W. DRYFE

Physical and Theoretical Chemistry Laboratory, Oxford University, South Parks Road, Oxford OX1 3QZ, Great Britain

Received 23 December 1994; revised 8 March 1995

The 'strongly implicit procedure' is shown to be a general, easy-to-use, stable and computationally efficient method of solving the mass transport equations necessary to predict transient voltammetric responses of electrode processes to which diffusion, convection and homogeneous chemical reaction may all contribute. The method is illustrated with a diversity of problems relating to electrodes of both micro- and milli-dimensions. In all cases excellent agreement with experiment and/or existing analytical or numerical theory is noted. Comparisons are made with alternative computational methods.

1. Introduction

The quantitative interpretation of voltammetric experiments requires the solution of sets of coupled partial differential equations which describe the processes of diffusion, convection and homogeneous kinetic decay in the vicinity of an electrode surface. Various numerical strategies have been proposed in this content [1, 2] to fulfil this need, most of which require substantial computational sophistication in order to achieve useful results. The purpose of the present article is to recommend the Strongly Implicit Procedure (SIP), invented by Stone [3] and subsequently very widely applied in nonelectrochemical applications [4–7]. SIP is a fast iterative method of great convenience to experimentalists due to its ready availability [8] in the form of a standard subroutine in the NAG Fortran Library (D03EBF) which permits valid results to be obtained without recourse to more than the most elementary computational aspects of numerical simulation. In particular we build on our success in solving steady-state problems [9] using SIP and show the approach to readily permit the solution of a variety of transient voltammetric problems.

Specifically, we consider first the response of a microband electrode to a potential step under diffusion only conditions. Existing analytical and numerical theory is used to demonstrate the veracity of the results. Second, the problem of mass transport to microband electrodes located in a rectangular channel flow is tackled and the relative merits of alternative computational approaches, notably the Hopscotch algorithm [10–13] and the Backwards Implicit (BI) method pioneered by Laasonen [14–16], are assessed particularly in terms of computational efficiency. Finally the use of SIP in solving transient problems involving homogeneous kinetics is illustrated by consideration of an ECE process, where the electrode and chemical reactions are coupled as shown, occurring at a microband channel electrode.

2. Theory

In the SIP a two dimensional partial differential equation is cast into finite difference form using an implicit approximation [1] so as to generate a set of simultaneous equations of five diagonal form:

$$a'_{i,j}p_{i,j-1} + b'_{i,j}p_{i-1,j} + c'_{i,j}p_{i,j} + d'_{i,j}p_{i+1,j} + e'_{i,j}p_{i,j+1} = q_{i,j} \quad (1)$$

which can be re-cast as a matrix equation

$$[A]\{p\} = \{q\}$$

where $\{p\}$ and $\{q\}$ are K-dimensional vectors of unknown and known elements, respectively, $\{q\}$ contains the boundary conditions and $[A]$ is a $K \times K$ matrix. The trick of SIP is to modify $[A]$ by the addition of a matrix $[B]$ such that $[A] + [B]$ is factorable into a lower $[L]$ and upper $[U]$ triangular matrix so that $[A] + [B] = [L][U]$. The equation

$$([A] + [B])\{p\} = \{q\} + [B]\{p\}$$

is solved iteratively

$$([A] + [B])\{p\}^{k+1} = \{q\} + [B]\{p\}^{k}$$

from a starting approximation $\{p\}^1$. How $[B]$ and $\{p\}^1$ are chosen and the specifics of the algorithm, including the determination of the iteration parameters, are discussed elsewhere [3–8]: however given the essentially ubiquitous availability of the NAG library such detail is unnecessary for the experimental electrochemist seeking to interpret their results. All that is necessary is first to identify the appropriate mass transport equations and boundary conditions pertaining to the problem of interest and second to cast them into finite difference form which is then rearranged into the style of equation (1) so permitting

* Author to whom all correspondence should be addressed.

0021-891X

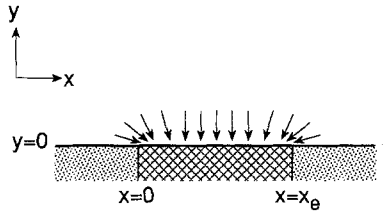

Fig. 1. Schematic diagram showing a microband electrode. The arrows represent the directions of diffusion to the electrode.

the elements of matrices $[A]$ and $\{Q\}$ to be specified for inclusion in the D03EBF subroutine. We next illustrate this exercise for the problems of interest as specified in the introduction.

First we examine the transient response of a microband electrode under diffusion only conditions if the electrode potential is stepped from a value at which no current flows to one corresponding to the transport limited discharge of a species, A:

$$A \pm e^- \longrightarrow B$$

The relevant mass transport equation describing the spatial distribution of A is

$$\frac{\partial a}{\partial t} = D\frac{\partial^2 a}{\partial y^2} + D\frac{\partial^2 a}{\partial x^2} \qquad (2)$$

where x and y are defined in Fig. 1, a is the concentration of species A and D its diffusion coefficient.

The boundary conditions pertinent to the problem of interest *after* the potential step has been applied are as follows:

$y = 0$	$0 < x < x_e$	$a = 0$
$y = 0$	$x < 0$	$\partial a/\partial y = 0$
$y = 0$	$x > x_e$	$\partial a/\partial y = 0$
$y \longrightarrow +\infty$	all x	$a = a_{bulk}$
all y	$x \longrightarrow -\infty$	$a = a_{bulk}$
all y	$x \longrightarrow +\infty$	$a = a_{bulk}$

where x_e is the electrode length. Note that the condition $a = 0$ corresponds to the transport–limited regime. To solve Equation 2 we adopt the finite difference grid shown in Fig. 2 which covers the x–y plane and has increments Δx and Δy in the x and y directions, respectively, so that

$y = j\Delta y \quad j = 0, 1, 2, \ldots, NJ$ where $\Delta y = nx_e/NJ$

$x = k\Delta x \quad k = -K_2, \ldots, -1, 0, 1, \ldots, K_1, \ldots, K_3$ where $\Delta x = x_e/K_1$

where calculations in the y direction extend n electrode lengths into the solution, $\alpha = (K_2/K_1)$ electrode lengths in the negative x direction and $\beta(= \{K_3/K_1\} - 1)$ electrode lengths in the positive x direction. For diffusion only problems, $\alpha = \beta$; however the general asymmetric grid is useful for calculations involving flow as will be described below.

The SIP method involves solving Equation 2 starting from an initial condition in which the cell is uniformly filled with A,

$$t = 0 \quad \text{all } x, \text{ all } y \quad a = a_{bulk}$$

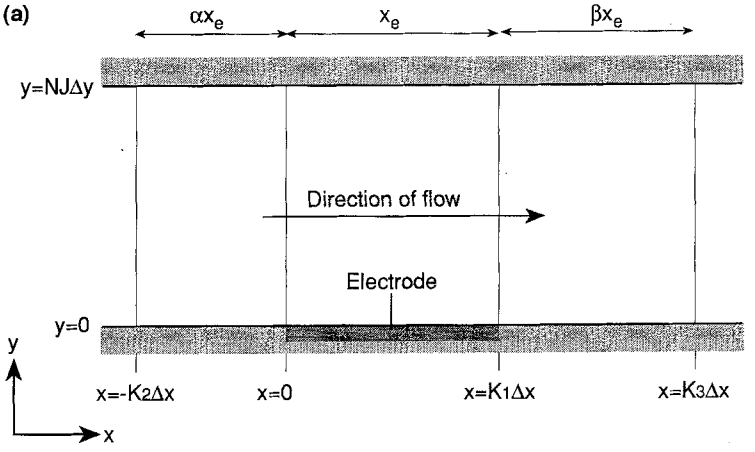

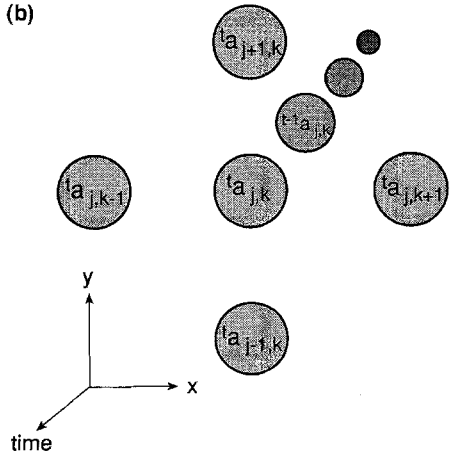

Fig. 2. (a) Finite-difference grid used for simulations. Note that there are NJ 'boxes' above the electrode, K_1 along the electrode, K_2 in the negative x direction and K_3 in total in the positive x direction. If convective flow is present it is in the positive x direction, as shown. (b) Network of matrix elements required in the SIP for the computation of the term ${}^t a_{j,k}$.

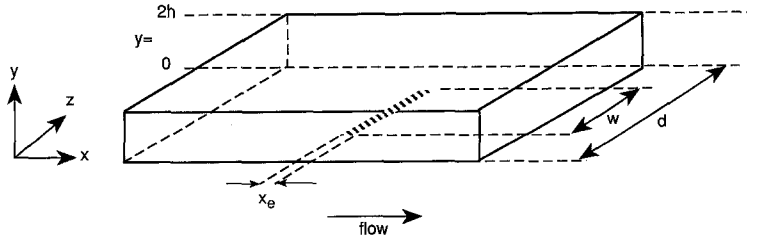

Fig. 3. Schematic diagram showing a microband channel electrode.

For $t > 0$ the boundary conditions previously identified are supplied. Time increments Δt are used with a counter T so that

$$t = t^*\Delta t \quad \text{for} \quad t^* = 0, 1, 2, \ldots, T$$

We use the symbol ${}^{t^*}a_{j,k}$ to denote the concentration of A at the coordinate (j,k). Equation 2 becomes

$$\frac{{}^{t+1}a_{j,k} - {}^{t}a_{j,k}}{\Delta t} = \frac{D}{(\Delta x)^2}({}^{t+1}a_{j,k+1} - 2^{t+1}a_{j,k} + {}^{t+1}a_{j,k-1}) + \frac{D}{(\Delta y)^2}({}^{t+1}a_{j+1,k} - 2^{t+1}a_{j,k} + {}^{t+1}a_{j-1,k})$$

which is readily cast into the form of Equation 1. This is solved using the SIP algorithm applied in the standard manner [8] and the current evaluated from the following expression

$$I = \frac{wFD[\mathrm{A}]_{\mathrm{bulk}}\Delta x}{\Delta y}\sum_{k=1}^{k=K_1} {}^{t}a_{1,k} \tag{3}$$

where w is the width of the microband electrode and F is Faraday's constant.

Next, we consider the transient response due to a potential step on a microband electrode located in a channel flow cell (Fig. 3). The pertinent mass transport equation becomes

$$\frac{\partial a}{\partial t} = D\frac{\partial^2 a}{\partial y^2} + D\frac{\partial^2 a}{\partial x^2} - v_x\frac{\partial a}{\partial x} \tag{4}$$

where v_x represents the solution velocity profile in the x direction. The latter is parabolic, provided one is considering laminar flow and that a sufficiently long lead in section is present for the flow to become fully developed [17]. Quantitatively,

$$v_x = v_0\left(1 - \frac{(h-y)^2}{h^2}\right) \tag{5}$$

where v_0 is the velocity at the centre of the channel and $2h$ is the channel depth (height). The boundary conditions pertinent to the problem of interest become

$y = 0$	$0 < x < x_e$	$a = 0$
$y = 0$	$x < 0$	$\partial a/\partial y = 0$
$y = 0$	$x > x_e$	$\partial a/\partial y = 0$
$y = 2h$	all x	$\partial a/\partial y = 0$
all y	$x \longrightarrow -\infty$	$a = a_{\mathrm{bulk}}$
all y	$x \longrightarrow +\infty$	$\partial a/\partial x = 0$

In finite difference form Equation 4 is given by

$$\frac{{}^{t+1}a_{j,k} - {}^{t}a_{j,k}}{\Delta t} = \frac{D}{(\Delta x)^2} \times ({}^{t+1}a_{j,k+1} - 2^{t+1}a_{j,k} + {}^{t+1}a_{j,k-1}) + \frac{D}{(\Delta y)^2}({}^{t+1}a_{j+1,k} - 2^{t+1}a_{j,k} + {}^{t+1}a_{j-1,k}) - \frac{v_x}{2\Delta x}({}^{t+1}a_{j,k+1} - {}^{t+1}a_{j,k-1})$$

which again is readily rearranged to the form of Equation 1, so permitting solution via the SIP. The current/time response is then again computed via Equation 3.

Finally, we turn to a consideration of potential step transients resulting from an ECE process at both micro- and milliband channel electrodes. This process is defined by the following reaction scheme in which the electroactive species, A, is first oxidized (reduced) to a species B which undergoes rapid decomposition to C. The latter then undergoes further electron transfer at the electrode:

$$\mathrm{A} \pm \mathrm{e}^- \longrightarrow \mathrm{B}$$

$$\mathrm{B} \xrightarrow{k} \mathrm{C}$$

$$\mathrm{C} \pm \mathrm{e}^- \longrightarrow \text{products}$$

The transient convective diffusion equations which describe the spatial distributions of A, B and C are

$$\frac{\partial a}{\partial t} = D\frac{\partial^2 a}{\partial y^2} + D\frac{\partial^2 a}{\partial x^2} - v_x\frac{\partial a}{\partial x} \tag{6}$$

$$\frac{\partial b}{\partial t} = D\frac{\partial^2 b}{\partial y^2} + D\frac{\partial^2 b}{\partial x^2} - v_x\frac{\partial b}{\partial x} - k.b \tag{7}$$

$$\frac{\partial c}{\partial t} = D\frac{\partial^2 c}{\partial y^2} + D\frac{\partial^2 c}{\partial x^2} - v_x\frac{\partial c}{\partial x} + k.b \tag{8}$$

where $a = [\mathrm{A}]$, $b = [\mathrm{B}]$, $c = [\mathrm{C}]$ and the diffusion coefficient, D, is assumed to be the same for all three molecules A, B and C. The pertinent boundary conditions are

$y = 0$	$0 < x < x_e$	$a = 0, \partial a/\partial y = -\partial b/\partial y, c = 0$
$y = 0$	$x < 0$	$\partial a/\partial y = \partial b/\partial y = \partial c/\partial y = 0$
$y = 0$	$x > x_e$	$\partial a/\partial y = \partial b/\partial y = \partial c/\partial y = 0$
$y = 2h$	all x	$\partial a/\partial y = \partial b/\partial y = \partial c/\partial y = 0$
all y	$x \longrightarrow -\infty$	$a = a_{\mathrm{bulk}}, b = c = 0$
all y	$x \longrightarrow +\infty$	$\partial a/\partial x = \partial c/\partial x = \partial b/\partial x = 0$

(9)

To solve Equations 6, 7 and 8 we again cast them into

finite difference form as illustrated by the following:

$$\frac{{}^{t+1}b_{j,k} - {}^{t}b_{j,k}}{\Delta t} = \frac{D}{(\Delta x)^2} \times ({}^{t+1}b_{j,k+1} - 2^{t+1}b_{j,k} + {}^{t+1}b_{j,k-1}) + \frac{D}{(\Delta y)^2}({}^{t+1}b_{j+1,k} - 2^{t+1}b_{j,k} + {}^{t+1}b_{j-1,k}) - \frac{v_x}{2\Delta x}({}^{t+1}b_{j,k+1} - {}^{t+1}b_{j,k-1}) - k^{t+1}b_{j,k+1}$$

Analogous equations may be written for a and c. These are solved using the strongly implicit procedure applied in the standard manner [8], solving first for a, then b and finally c, the concentration profiles being 'linked' through the boundary conditions (9), which dictate this sequence of solution. The current is then evaluated from the following expression

$$I = \frac{wFD[\mathrm{A}]_{\mathrm{bulk}}\Delta x}{\Delta y}\sum_{k=1}^{k=K_1}(a_{1,k} + c_{1,k}) \qquad (10)$$

for different flow rates and cell/electrode geometries.

All programs were written in Fortran 77 and executed on a Silicon Graphics Indigo [2].

3. Results and discussion

We consider first the theoretical results obtained for potential step transients measured at microband electrodes under diffusion only conditions and note that approximate analytical solutions have been derived for this problem. In particular the current at sufficiently short times is given by the following equation [18, 19] originally due to Oldham [18] valid for $\theta < 2$.

$$I = nFa_{\mathrm{bulk}}D\left(\frac{A}{\pi^{1/2}D^{1/2}t^{1/2}} + \frac{P}{2}\right)$$

$$I = nFDa_{\mathrm{bulk}}w\left(\frac{1}{\pi^{1/2}\theta^{1/2}} + 1\right)$$

where $\theta = Dt/x_e^2$ and P is the electrode perimeter ($\sim 2w$ for a microband electrode). The long time behaviour has been described by Aoki [20] as

$$I = nFa_{\mathrm{bulk}}Dwf(\theta)$$

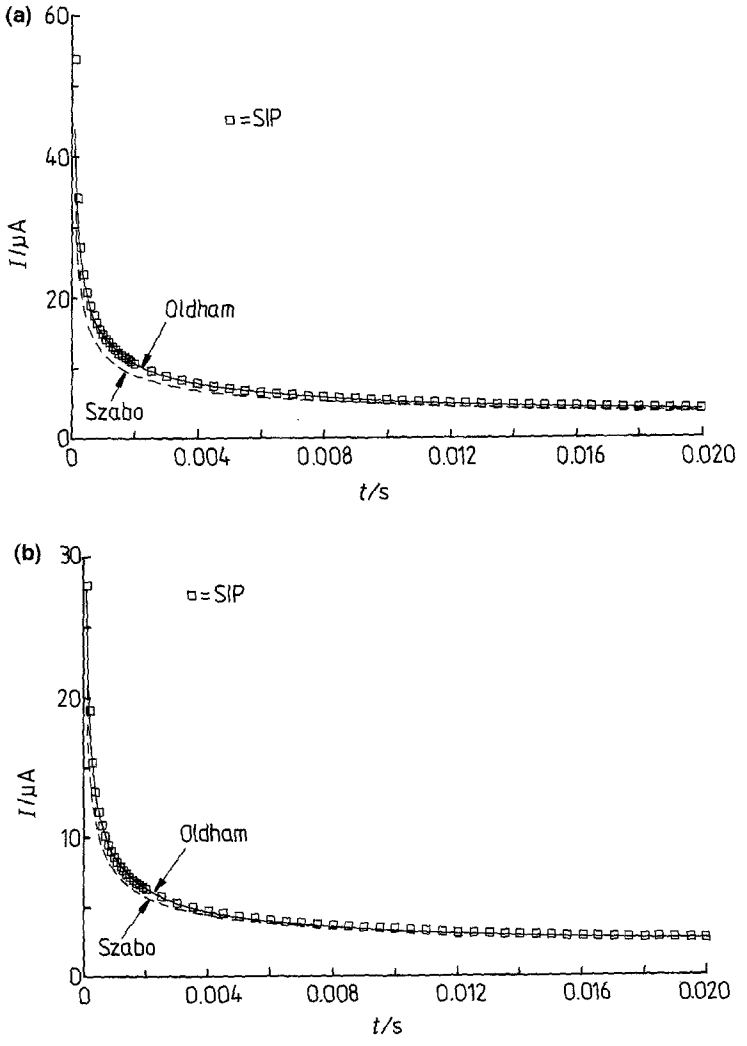

Fig. 4. SIP simulated transients describing the current flowing due to a potential step at microband electrodes ((a) $x_e = 33\,\mu$m, $w = 0.522$ cm and (b) $x_e = 20\,\mu$m, $w = 0.5$ cm) under diffusion only conditions. The following parameters were used in the simulations: (a) $a_{\mathrm{bulk}} = 1.09 \times 10^{-6}$ mol cm^{-3}, $D = 1.75 \times 10^{-5}$ cm^2 s^{-1}, $nx_e = 0.002$ cm and (b) $a_{\mathrm{bulk}} = 1.00 \times 10^{-6}$ mol cm^{-3}, $D = 2 \times 10^{-5}$ cm^2 s^{-1}, $nx_e = 0.0025$ cm. Also shown on the Figures are the transients predicted by the analytical equations of Oldham and Szabo [15, 18].

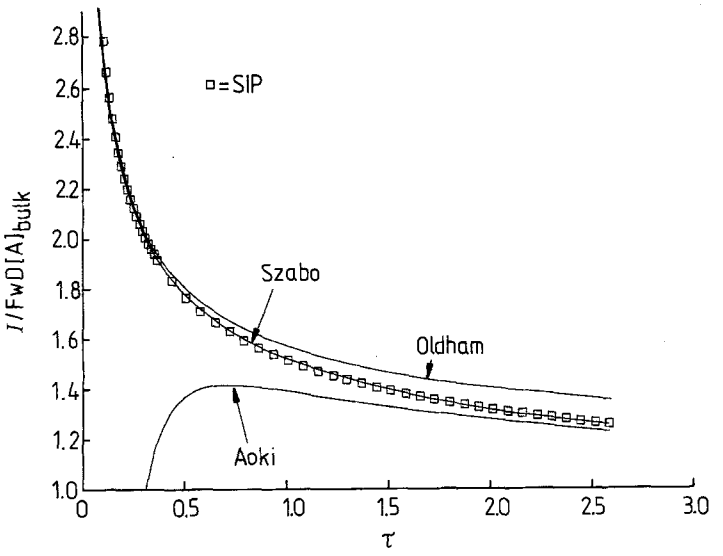

Fig. 5. A SIP simulated current transient induced by a potential step at a short microband electrode of dimensions $x_e = 4\,\mu m$ and $w = 0.364$ cm under diffusion only conditions. The following parameters were used in the simulations: $D = 2.3 \times 10^{-5}\,cm^2\,s^{-1}$, $a_{bulk} = 1.14 \times 10^{-6}$ mol cm^{-3} and $nx_e = 0.0024$ cm. Also shown on the Figure are the transients predicted by the approximate analytical equations of Oldham [15], Szabo [18] and Aoki [17].

where

$$f(\theta) = 2\pi[(\ln(\theta) + 3)^{-1} - 0.577(\ln(\theta) + 3)^{-2} - 1.312(\ln(\theta) + 3)^{-3}]$$

and Szabo [21] as

$$I = nFDa_{bulk}w\left[\frac{\pi e^{-2\sqrt{\pi\theta}/5}}{4\sqrt{\pi\theta}}\right] + \frac{\pi}{\ln[(64e^{-\gamma}\theta)^{1/2} + e^{5/3}}$$

The latter expression is valid for $\theta > 0.4$. Figure 4 shows the results of SIP simulations for electrodes of size $x_e = 20\,\mu m$ and $33\,\mu m$, respectively. The other parameters used in the simulations are specified in the figure legend. For the purposes of SIP simulation a grid size of 500×500 was found to give converged currents to within three significant figures for times greater than 1 ms. The real time duration of the two transients corresponds to $\theta \ll 2$ corresponding to the situation where the Oldham equation should be valid. The transients predicted by this equation are additionally shown in Fig. 4 and excellent agreement may be noted. The Szabo equation in contrast is, as expected for the time domain considered, seen to give poor, but not entirely unacceptable agreement, except towards the longer time portions of the transients. This behaviour should be contrasted with that shown in Fig. 5 which gives simulated results for a much shorter electrode of length, $x_e = 4\,\mu m$. The x axis of this plot is given in terms of the normalized time, θ. The different regions of applicability of the approximate analytical solutions are now evident. In particular the success of the Szabo equation at long times ($\theta > 0.4$) is essentially quantitative whilst the increasing breakdown of the Oldham equation at longer times is also clear. It has been suggested [22] that the Oldham equation is accurate to within 5% for $\theta < 2$. Figure 5 shows that this is unrealistically optimistic. Figure 5 also includes the long time asymptote derived by Aoki; this is seen to approach the

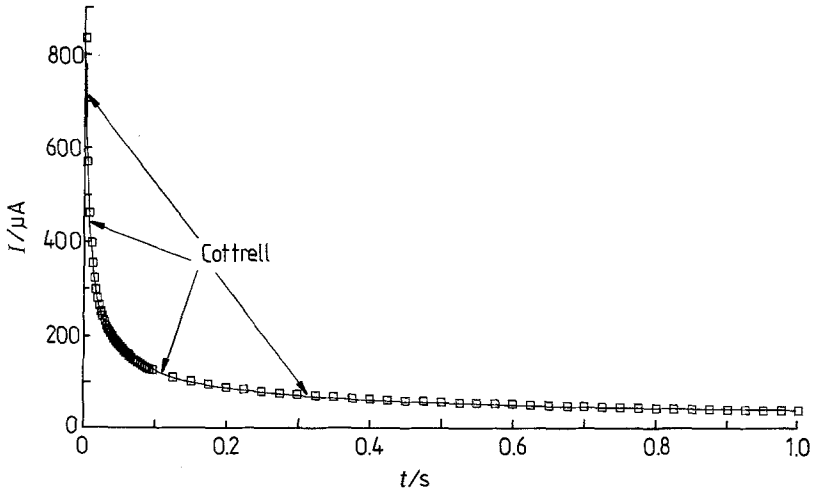

Fig. 6. SIP simulated current transient induced by a potential step at a band electrode of dimensions $x_e = 4$ mm and $w = 4$ mm under diffusion only conditions. The following parameters were used in the simulations: $D = 2.0 \times 10^{-5}\,cm^2\,s^{-1}$ and $a_{bulk} = 1.0 \times 10^{-6}$ mol cm^{-3}. Also shown on the Figure is the behaviour predicted by the Cottrell equation [20].

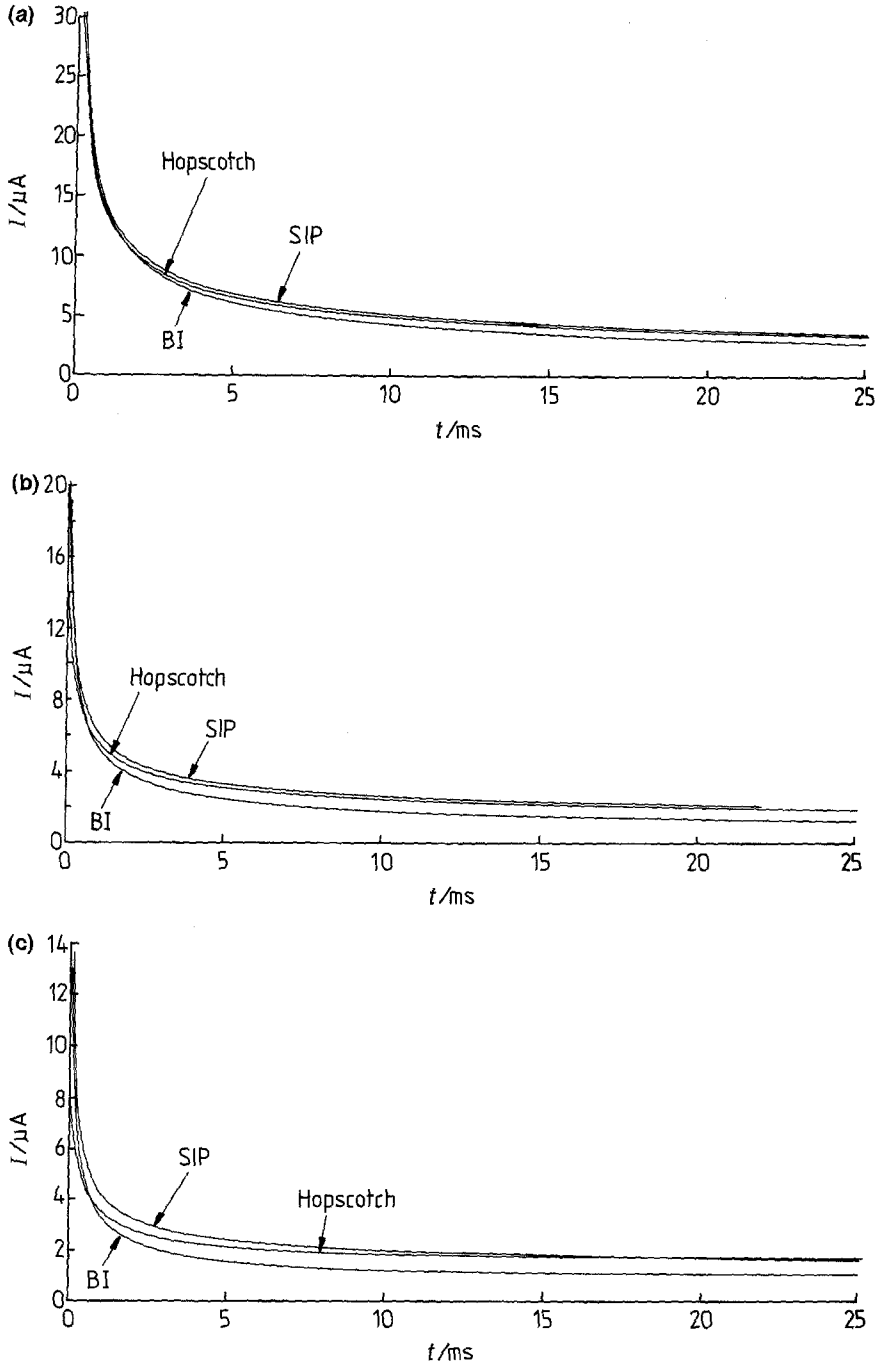

Fig. 7. Simulated SIP transients for channel microband electrodes of different sizes exposed to varying solution flow rates (V_f/cm^3 s^{-1}) as follows: (a) $x_e = 33\,\mu$m and $V_f = 2.34 \times 10^{-3}$, (b) $x_e = 13\,\mu$m and $V_f = 5.79 \times 10^{-3}$, (c) $x_e = 4\,\mu$m and $V_f = 1.36 \times 10^{-2}$. The following parameters were used in the simulations: $D = 1.75 \times 10^{-5}$ cm^2 s^{-1}, $a_{bulk} = 1.09 \times 10^{-6}$ mol cm^{-3} and $2h = 0.044$ cm. The corresponding Peclet numbers, giving a measure of the relative contributions of convection and diffusion, are (a) $Pe = 28$; (b) $Pe = 3.4$.

authentic behaviour only at very long times. Finally, Fig. 6 depicts a simulation for an $x_e = 4$ mm electrode. This is sufficiently large for diffusional edge effects to be effectively negligible and the transient quantitatively follows the behaviour predicted by the Cottrell equation [23] for semi-infinite diffusion in one-dimension.

We examine next transients recorded for microband electrodes located in a channel flow cell and subject to convective mass transport in addition to that from diffusion. Again the case of a potential step from a value corresponding to no current flow to one which the transport-limited current was passed was considered. Channel microband electrodes of length (x_e) 8 μm, 13 μm and 33 μm located in a channel of dimensions $2h = 0.044$ cm, $d = 0.6$ cm and $w = 0.522$ cm were simulated for $D = 1.75 \times 10^{-5}$ cm^2 s^{-1} (corresponding to the literature value [24] for the diffusion coefficient of p-chloranil in acetonitrile solution) and a bulk concentration of 1.09×10^{-6} mol cm^{-3} for the electroactive species; it was found that a finite difference grid size of 500 × 1000 was sufficient to give convergence to three significant figures for flow rates in the range 1×10^{-3} to 1×10^{-1} cm^3 s^{-1}. Figure 7 shows the results of the SIP simulations in each case. The simulation of the microband channel transients was also examined using both the Hopscotch algorithm, which has been shown to generate results in excellent

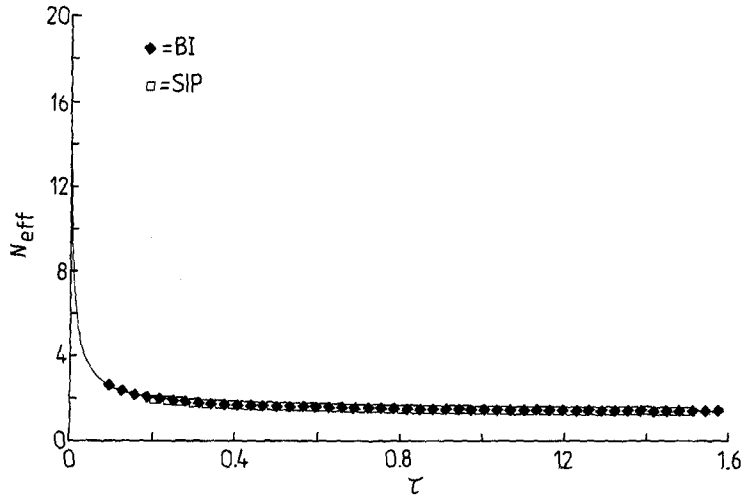

Fig. 8. SIP simulated current transient induced by a potential step at a channel electrode of dimensions $x_e = 4\,mm$, $w = 4\,mm$, for an ECE-type electrode process with $k = 1\,s^{-1}$. The following parameters were used in the simulations: $d = 6\,mm$, $a_{bulk} = 1 \times 10^{-6}\,mol\,cm^{-3}$, $D = 2 \times 10^{-5}\,cm^2\,s^{-1}$ and $V_f = 1 \times 10^{-2}\,cm^3\,s^{-1}$. $Pe = \sim 14200$.

agreement with experiment [25] and the BI method (see Introduction) which can be used to solve the problem provided the effects of axial diffusion are neglected and the term $D(\partial^2 a/\partial x^2)$ is omitted from Equation 4. The grid sizes required to achieve convergence to three significant figures for the Hopscotch method were similar to those employed for SIP. The following values (Table 1) were used as time increments and number of steps (T), respectively:

Table 1

Electrode size	*Time increment*/s^{-1}	*Simulation time*	*No. of steps*
4 μm	40000	20 ms	800
20 μm	20000	20 ms	400
33 μm	10000	20 ms	200
4 mm	1000	1 s	1000

Inspection of the transients shown in Fig. 7 reveals that there is excellent agreement between the two current–time curves computed from SIP and Hopscotch. At short times there is also correspondence with the BI transient although in general the latter tends to underestimate the current because of the neglect of axial (x direction) diffusion. The relative merit of the SIP over the Hopscotch approach, in addition to the advantages of simplicity and ease-of-use identified earlier, can be noted if a comparison of the amounts of CPU time required by the different simulation methods to produce a single, converged transient at a typical flow rate is made: SIP ~2–3 h, Hopscotch ~10 h and BI ~10 min. The benefits of SIP over Hopscotch are significant although if the experimental conditions to be modelled permit the neglect of axial diffusion the BI method is optimally efficient owing to the fact that the BI method relies only on *vector calculations* rather than *matrix iterations*.

Last we turn to the third example of the use of SIP for modelling transients and consider the current/time

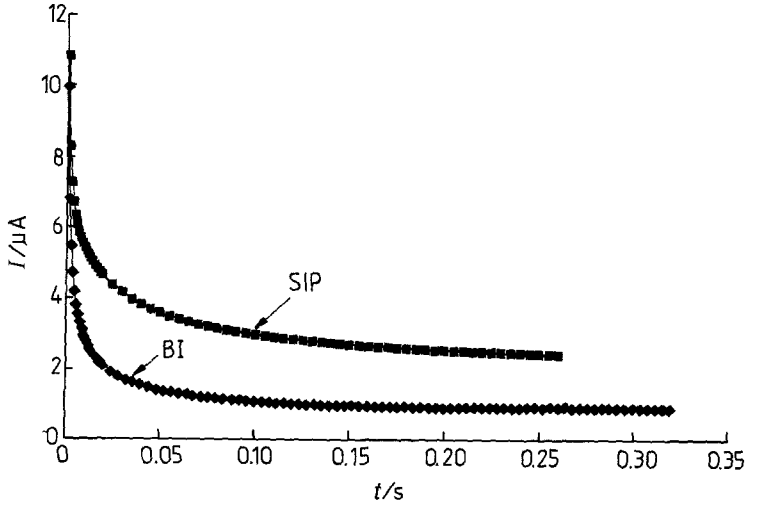

Fig. 9. SIP simulated current transient induced by a potential step at a channel microband electrode of dimensions $x_e = 30\,\mu m$, $w = 4\,mm$ for an ECE-type electrode process with $k = 100\,s^{-1}$. The following parameters were used in the simulations: $D = 2.0 \times 10^{-5}\,cm^2\,s^{-1}$, $a_{bulk} = 1.0 \times 10^{-6}\,mol\,cm^{-3}$ and $2h = 0.04\,cm$.

behaviour resulting from a potential step at a channel electrode where the electrode process constitutes an ECE reaction. Figure 8 shows the SIP transient for a large (x_e= 4 mm) channel electrode computed for a solution flow rate of 1×10^{-2} cm^3 s^{-1}, a first order homogeneous rate constant (k) for the conversion of B to C (see above) of 1 s^{-1}, and a cell geometry of 2 $h = 0.04$ cm and $d = 0.6$ cm. The transient is shown in the form of a plot of the effective number of electrons transferred, N_{eff}, which varies between unity (for $k = 0$) and 2 (for $k \rightarrow \infty$) against a dimensionless time parameter, τ, previously defined as appropriate for channel electrodes of other than microelectrode dimensions [16]:

$$\tau = t\left(\frac{4Dv_o^2}{h^2x_e^2}\right)^{1/3}$$

Also shown in Fig. 8 is the corresponding transient computed using BI theory with the neglect of axial diffusion (as above). The agreement between the two transients is quantitative to better than 0.1% as is expected for an electrode of the size examined [25, 26]. In contrast Fig. 9 shows the corresponding transient for an electrode with $x_e = 30\,\mu$m and $k = 100$ s^{-1}, all other parameters being unchanged from those given in Fig. 8. In this case there is a marked contrast between the two demonstrating the significant contribution from axial diffusion in the case of the microelectrode geometry. Both Figs 8 and 9 demonstrate the viability of the SIP approach for processes involving coupled homogeneous kinetics. It should be noted that if applicable the BI method is again substantially faster than the SIP method: the transients in Figs 8 and 9 required about 8–9 h of CPU time in the case of SIP as opposed to about 30 min for BI. However in the case of microelectrodes with convection, the SIP is the method of choice since the neglect of x direction diffusion is unrealistic and we have found the Hopscotch approach to be prohibitively expensive in CPU time if appropriately converged results are to be obtained.

4. Conclusions

The SIP is readily available for use in the simulation of voltammetric current/time transients through its appearance as the NAG Library Subroutine D03EBF. As such it is recommended as a highly convenient method for the computer modelling of experimental electrochemical data since it requires simply the formulation of the problem of interest in terms of mass transport equations, boundary conditions and their finite-difference equivalents. The need for generating elaborate computer code for the simulation itself is obviated.

This paper has shown that the SIP may be effectively applied to problems in which diffusion, convection and homogeneous kinetics may significantly contribute, and to electrodes of both micro and traditional dimensions. We anticipate its widespread adoption by experimental (and other) electrochemists. Note further that the extension to include non-uniform grids should render the application of SIP even more computationally efficient.

Acknowledgements

We thank EPSRC for financial support (Grant GR/H99288), the NERC for a studentship for RAWD and the Dyke Exhibition Foundation for an award to JAA.

References

[1] L. Lapidus and G. F. Pinder, 'Numerical Solution of Partial Differential Equations in Science and Engineering', J. Wiley & Sons, New York (1982).
[2] D. Britz, 'Digital Simulation in Electrochemistry', Springer-Verlag, Berlin (1988).
[3] H. L. Stone, SIAM *J. Numer. Anal.* **5** (1968) 530.
[4] K.-H. Chen and R. H. Pletcher, *AIAA J.* **29** (1991) 1241.
[5] R. W. Walters, D. L. Dwoyer and H. A. Hassan, *ibid.* **24** (1986) 6.
[6] G. E. Schneider and M. Zedan, *Numerical Heat Transfer* **4** (1981) 1.
[7] M. Zedan and G. E. Schneider, *ibid.* **8** (1985) 537.
[8] NAG Fortran Library Mark 13, National Algorithms Group, Oxford, vol. 3, section D03EPF, p. 3.
[9] R. G. Compton, R. A. W. Dryfe, R. G. Wellington and J. Hirst, *J. Electroanal. Chem.* **383** (1995) 13.
[10] A. R. Gourlay and G. R. McGuire, *J. Inst. Math. Appl.* **7** (1971) 216.
[11] D. Shoup and A. Szabo, *J. Electroanal. Chem.* **160** (1984) 17.
[12] R. M. Wightman and C. Amatore, *ibid.* **267** (1989) 33.
[13] P. Pastore, F. Magno, J. Lavagnini and C. Amatore, *ibid.* **301** (1991) 1.
[14] P. Laasonen, *Acta Math.* **81** (1949) 30917.
[15] J. L. Anderson and S. Moldoveanu, *J. Electroanal. Chem.* **179** (1984) 107.
[16] A. C. Fisher and R. G. Compton, *J. Phys. Chem.* **95** (1991) 7538.
[17] V. G. Levich, 'Physicochemical Hydrodynamics', Prentice-Hall, Englewood Cliffs, NJ (1962).
[18] K. Oldham, *J. Electroanal. Chem.* **122** (1981) 1.
[19] K. Aoki, K. Tokuda and H. Matsuda, *Denki Kagaku* **54** (1986) 1010.
[20] K. Aoki, K. Tokuda and H. Matsuda, *J. Electroanal. Chem.* **230** (1987) 61.
[21] A. Szabo, D. K. Cope, D. E. Tallman, P. M. Kovach and R. W. Wightman, *ibid.* **217** (1987) 417.
[22] K. Aoki, *Electroanalysis* **5** (1993) 1.
[23] F. G. Cottrell, *Z. Physik. Chem.* **42** (1902) 385.
[24] M. E. Peover, *J. Chem. Soc.* (1962) 4540.
[25] R. G. Compton, R. A. W. Dryfe, J. A. Alden, N. V. Rees, P. J. Dobson and P. A. Leigh, *J. Phys. Chem.* **98** (1994) 1270.
[26] R. G. Compton, R. G. Wellington, P. J. Dobson and P. A. Leigh, *J. Electroanal. Chem.* **370** (1994) 129.